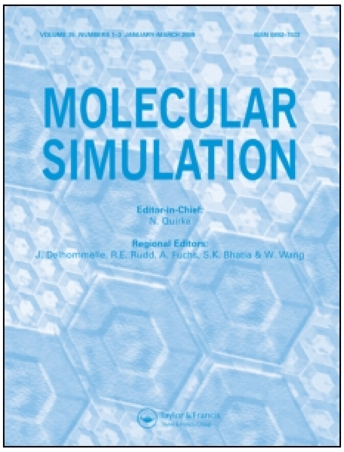

Molecular Simulation
Publication details, including instructions for authors and subscription information:
http://www.informaworld.com/smpp/title~content=t713644482

Static and dynamic properties of ionic liquids

T. Koishi[a]; S. Fujikawa[b]
[a] Department of Applied Physics, University of Fukui, Fukui, Japan [b] Interfacial Nanostructure Research Laboratory, RIKEN, Saitama, Japan

To cite this Article Koishi, T. and Fujikawa, S.(2010) 'Static and dynamic properties of ionic liquids', Molecular Simulation, 36: 15, 1237 — 1242, First published on: 02 November 2010 (iFirst)

To link to this Article: DOI: 10.1080/08927020903536358

URL: http://dx.doi.org/10.1080/08927020903536358

Molecular Simulation
Vol. 36, No. 15, December 2010, 1237–1242

Taylor & Francis
Taylor & Francis Group

Static and dynamic properties of ionic liquids

T. Koishi[a]* and S. Fujikawa[b]

[a]*Department of Applied Physics, University of Fukui, 3-9-1 Bunkyo, Fukui 910-8507, Japan;* [b]*Interfacial Nanostructure Research Laboratory, RIKEN, Wako, Saitama 351-0198, Japan*

(*Received 1 September 2009; final version received 7 December 2009*)

We performed molecular dynamics (MD) simulations of ionic liquids composed of 1-butyl-3-methylimidazolium ([bmim]) cation with PF_6, NO_3 and Cl anions to determine their static and dynamic properties. Large-scale simulation of 4096 ion pairs (131,072 particles in [bmim]PF_6) was performed to estimate the system-size dependence of the static and dynamic properties. The diffusion constant, which is 100 times smaller than that of a normal liquid such as water, was estimated from long-time simulations. We also performed non-equilibrium MD simulations to determine the electrical conductivity. We obtained a nonlinear relationship between the electrical current and external electric field strength.

Keywords: ionic liquid; molecular dynamics simulation; structure; dynamic properties; non-equilibrium molecular dynamics

1. Introduction

Ionic liquids are liquid organic salts at room temperature. The most characteristic property of ionic liquids is that their melting temperatures are much lower than those of typical salts, e.g. NaCl. Recently, researchers have extensively investigated their applications as clean solvents and electrolytes for batteries and their use in electrosynthesis.

Canongia Lopes et al. [1] developed the force field of ionic liquids composed of 1-alkyl-3-methylimidazolium cation with PF_6, NO_3 and Cl anion system, which was one of the most widely used ionic liquid families. This force field allows us to perform all-atom molecular dynamics (MD) simulations in which each particle of cation and anion of the ionic liquids can be considered. They determined energy profiles and the distribution of atomic charges by the *ab initio* calculation. The force field was validated by comparing simulation and experimental results with both the solid-state crystallographic data and liquid-state densities. The relative deviations of the densities from the experimental results were 1–5%.

Many MD simulations of the ionic liquids have been performed using the all-atom force field [2–4]. The computational cost is very high because cations and anions can contain many atoms. Therefore, large-scale and long-time MD simulations have not been performed. The pairs of ion pair number and mean square displacement (MSD) length of previous MD simulations are (300, 2.8 ns) [5], (400, 1.0 ns) [6], (200, 500 ps) [7], (216, 500 ps) [8] and (125, 30 ns) [9]. In addition, systematic studies of the correlations between the static structures and transport properties of ionic liquids have not been investigated until recently.

Kowsari et al. [10,11] estimated dynamic properties of ionic liquids in 2008 and 2009. They performed MD simulations to study twelve 1-alkyl-3-methylimidazolium-based ionic liquids (alkyl = methyl, ethyl, propyl and butyl) with PF_6, NO_3 and Cl anions and derived diffusion constants, electrical conductivities and viscosities. The MSD and the velocity auto-correlation function (VACF) were derived to estimate the diffusion constant. Theoretically, the diffusion constant can be calculated from the slope of the MSD and the integration of the VACF using the Einstein relation and Green–Kubo formula, respectively. Their results reasonably agreed with the experimental results; however, they suggested that longer simulations in the range of approximately 5–10 ns may be required to obtain better results. The diffusion coefficients calculated using the Green–Kubo formula were very sensitive to the selected upper time limits of the VACF integrals [10]. The electrical conductivity was calculated from the Nernst–Einstein and Green–Kubo formulae, and the viscosity was also determined from the Stokes–Einstein relation [11]. Electrical conductivities obtained by them were lower than the experimental results while those of the viscosity estimates were higher than the experimental results. They calculated electrical conductivities from the diffusion constant with the Nernst–Einstein relation and the integration of the electric current auto-correlation function with the Green–Kubo formula. In summary, they determined three electrical conductivities for each system from the MSDs and the VACFs with the Nernst–Einstein relation and from the electric

---

*Corresponding author. Email: koishi@polymer.apphy.u-fukui.ac.jp

ISSN 0892-7022 print/ISSN 1029-0435 online

DOI: 10.1080/08927020903536358
http://www.informaworld.com

current auto-correlation function with the Green–Kubo formula. The relative deviations of these results were very widely distributed from 6 to 65%. Their results disclosed the difficulty of estimating the electrical conductivity with the MD simulation.

In this study, we performed MD simulations for ionic liquids composed of 1-butyl-3-methylimidazolium ([bmim]) cation with PF_6, NO_3 and Cl anions to investigate their structures and dynamic properties, including their diffusion constants and electrical conductivities. The two system sizes, 216 and 4096 ion pairs, were employed to obtain the system-size dependence of the structures and the diffusion constants of the cations and anions. Long-time MD simulations over a span of 20–30 ns were performed to adapt to the slow dynamics of the ionic liquids and to estimate more accurate diffusion constants. We also performed non-equilibrium molecular dynamics (NEMD) simulations to calculate the electrical conductivities. In the estimation of the electrical conductivities, NEMD can eliminate the uncertainties of the integration of the electric current auto-correlation function, which includes the cut-off error of the integration. We were able to derive the electrical conductivities from the NEMD simulations more effectively than from the Green–Kubo integration. We used a special-purpose computer MDGRAPE-3 for the large-scale and long-time MD simulations. The MDGRAPE-3 accelerated MD simulations 10–100 times faster than general-purpose computers [12–14].

2. Simulation method

The force field used in this study is from the all-atom force field developed by Canongia Lopes et al. [1] based on the AMBER and OPLS force fields

$$\begin{aligned} U = {} & \sum_{\text{bonds}} k_b(r - r_0)^2 + \sum_{\text{angles}} k_a(\theta - \theta_0)^2 \\ & + \sum_{\text{dihedrals}} \sum_{n} \frac{V_n}{2}\{1 + \cos(n\phi - \gamma)\} \\ & + \sum\sum_{i<j} \left[4\varepsilon \left\{ \left(\frac{\sigma}{r_{ij}}\right)^{12} - \left(\frac{\sigma}{r_{ij}}\right)^{6} \right\} + \frac{z_i z_j}{r_{ij}} \right]. \end{aligned} \tag{1}$$

The first three terms represent the bond stretching, bond angle and dihedral angle interactions of the covalent bonds, respectively. The last term, which includes the van der Waals (Lennard-Jones) and Coulomb potentials, describes the interactions between the non-bonded atom pairs. Equation (1) describes the intramolecular interaction of the cations and the intermolecular interactions of the cation–cation and cation–anion pairs. The rigid-body model, which we used for the anion molecules, included two terms, a Lennard-Jones term and a Coulomb term. The bond lengths and the bond angles were fixed for the calculation of the anion molecules. We calculated the trajectory of the anion molecules using the Euler equation.

The MD simulation was performed at constant-volume and -temperature ($T = 313$ K) conditions. We determined the densities of the systems from the literature [1]. The constant-temperature MD was performed by the velocity scaling method. We integrated the equations of motion using the multiple time-step algorithm RESPA [15]. The time integrations for the rotational motion of rigid molecules were performed using a time-reversible algorithm [16]. We set the MD time step of the bond and angle integrations at 0.5 fs, that of the torsion integrations at 1.0 fs and that of the non-bonded integrations at 2.0 fs. The periodic boundary condition was applied in all three spatial dimensions. The long-range charge–charge interaction between water molecules was calculated using the Ewald method.

We performed NEMD simulations to obtain the DC electrical conductivities. An external electric field was applied to the system as shown schematically in Figure 1. We derived the electrical conductivity from the averaged ion velocity yielded by the external electric field. The NEMD method gave us the electrical conductivities more effectively than the equilibrium MD (EMD) method in which the electrical conductivity is calculated from the integration of the electric current auto-correlation function.

We used a special-purpose computer MDGRAPE-3, developed by Taiji et al. [12–14] in RIKEN, to reduce the simulation time. It accelerates force calculations in MD simulations. The peak performance of the chip was equivalent to 180 Gflops at 250 MHz. We used 16 MDGRAPE-3 boards to perform MD simulation of the largest system. The peak performance of a MDGRAPE-3 board, which contains 12 MDGRAPE-3 chips, was 2.16 Tflops.

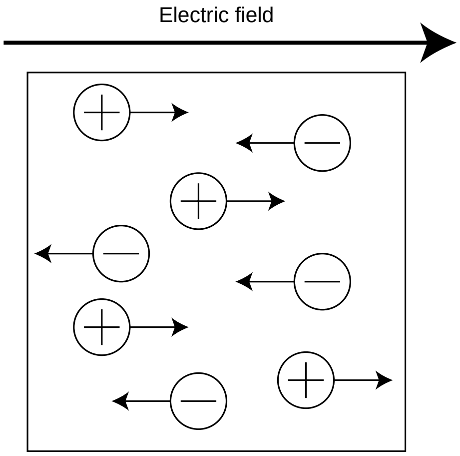

Figure 1. Schematic of NEMD in which an external field is applied.

MDGRAPE-3 handled three force calculations: (1) the real-space part of the long-range charge–charge interaction, (2) the van der Waals interaction and (3) the reciprocal-space part of the long-range charge–charge interactions. Other computationally less intensive calculations were handled by a host computer, including the updating of particle positions and the evaluation temperatures.

3. Results and discussion

3.1 Structure

We investigate the liquid structure through the radial distribution function, $g(r)$. This function shows the probability of the existence of a particle between r and $r+\mathrm{d}r$ as

$$g(r)=\frac{n(r)}{4\pi r^2\,\mathrm{d}r\rho}, \tag{2}$$

where $n(r)$ is the number of particles between r and $r+\mathrm{d}r$ and ρ is the number density. We calculated the radial distribution functions of the imidazolium (polar) part and the butyl (non-polar) part of the cation and the anion. The position of each part of the cation and anion was defined as their centre of mass. Figure 2 shows the system-size dependence of the radial distribution functions. In this figure, the symbol 'im' indicates the imidazolium part and 'bu' indicates the butyl part of the cation. The radial distribution functions for the system with 216 ion pairs were almost the same as those for the system with 4096 ion pairs. The system-size dependence of the radial distribution functions is very small in this system.

Figure 3 shows the radial distribution functions of [bmim]PF_6, [bmim]NO_3 and [bmim]Cl. The trend of the first peak height of the im–anion was [bmim]Cl $>$ [bmim]NO_3 $>$ [bmim]PF_6. It corresponded to an inverse correlation of the anion size as $PF_6 > NO_3 > Cl$. The order of the spread of the first peak of the im–im was [bmim]Cl $>$ [bmim]NO_3 $>$ [bmim]PF_6. This trend was consistent with that of the first peak height, meaning that the space in which the cations existed was widely distributed when the anion size was small.

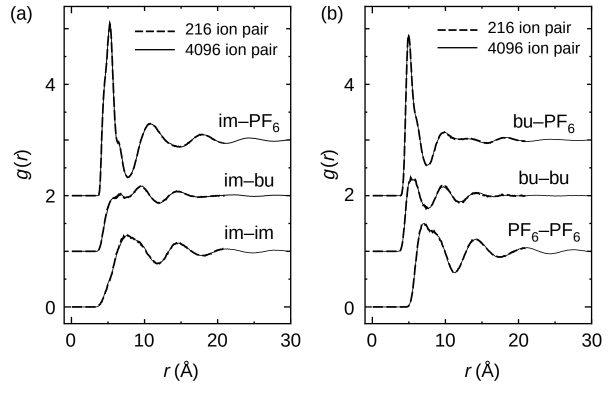

Figure 2. Radial distribution functions, $g(r)$, of [bmim]PF_6 at 216 and 4096 ion pairs. The symbol 'im' means an imidazolium part and 'bu' means a butyl part of the cation.

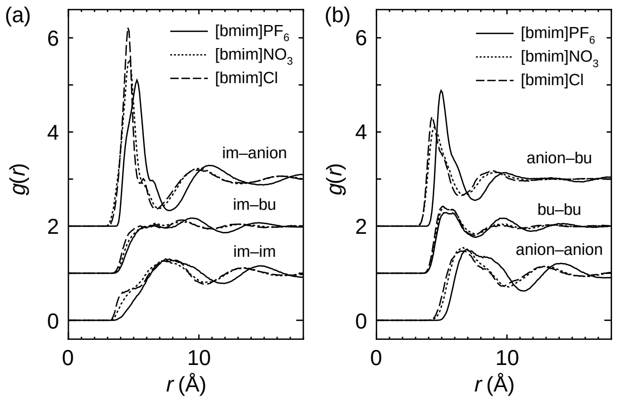

Figure 3. Radial distribution functions, $g(r)$, of [bmim]PF_6, [bmim]NO_3 and [bmim]Cl. The symbol 'im' means an imidazolium part and 'bu' means a butyl part of the cation.

3.2 Diffusion constant

We performed 30 and 20 ns MD simulations to calculate the MSD with 216 and 4096 ion pair systems, respectively. The MSDs of lengths of 20 and 10 ns were obtained for each system. In total, we determined 500 MSDs, the origins of which were shifted every 10 ps and averaged to obtain the MSDs for the calculation of the diffusion constant. Figure 4 displays the results. The slopes of the MSD are close to 1 over the range of 10–20 ns (Figure 4(b)). It indicates that the dynamics of ions are diffusive over the range. We also estimated the time dependence of the diffusion constants, as shown in Figure 5. In this figure, we calculated each point $D(t)$ from the slope of the MSDs over a range of t to $t+\Delta t$, with $\Delta t = 1$ ns; this range included 100 data points. The slope of the MSDs was nonlinear over the range of 0–10 ns, and $D(t)$ gradually decreased. $D(t)$ fluctuated over the range of 10–20 ns. Then, we determined that the diffusion constant of the cation was about $5\times10^{-12}\,\mathrm{m}^2/\mathrm{s}$ and that of the anion was about $3\times10^{-12}\,\mathrm{m}^2/\mathrm{s}$. The above results suggest that the length of the MSD requires over 10 ns in [bmim]PF_6 to estimate the accurate diffusion constant. The system-size effect of MSDs of 216 and 4096 ion pair systems is not large, because both MSDs converge at almost the same values. To estimate more detailed size effect of the diffusion constant, larger and longer simulations are required.

Figure 6 shows the MSDs of [bmim]PF_6, [bmim]NO_3 and [bmim]Cl. Table 1 lists the diffusion constants derived from the slope of these MSDs. The slopes of [bmim]PF_6 and [bmim]NO_3 are sufficiently close to 1, but that of [bmim]Cl is not enough. Therefore, the diffusion constant of [bmim]Cl may be overestimated and the actual diffusion constant must be smaller. The anion dependences of the

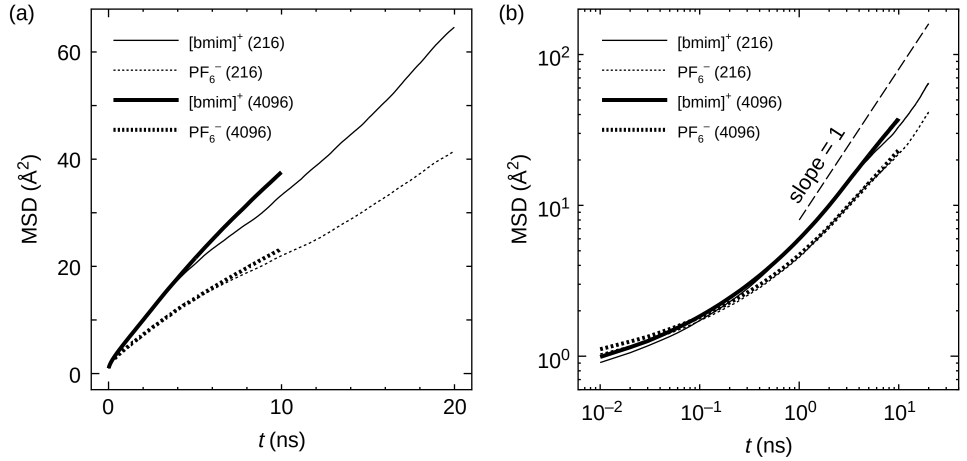

Figure 4. (a) MSDs of cations and anions of [bmim]PF_6 at 216 and 4096 ion pairs and (b) their log–log plot with the line of slope 1.

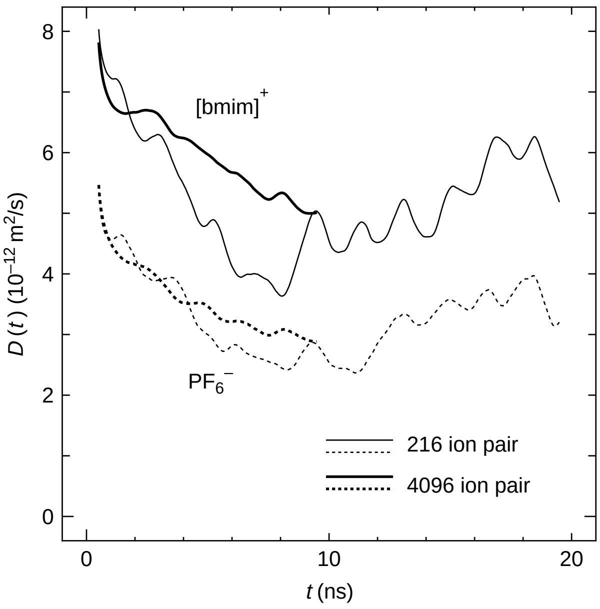

Figure 5. Time dependence of the diffusion constants, $D(t)$. Each point of $D(t)$ is calculated from the slope of the MSD at the range from t to $t+\Delta t$, with $\Delta t = 1$ ns. This range includes 100 data points.

diffusion constants varied greatly depending on the anion. The trend of the diffusion constants did not correspond to that of the peak height of $g(r)$ of the im–anion, as shown in Figure 3. In particular, the diffusion constants of [bmim]NO_3 were large. The reason for this cannot be clarified from the structural results of the radial distribution functions.

3.3 Electrical conductivity

In the NEMD simulations, we applied an external electric field to all cations and anions. The range of the applied force magnitude was from 0.02×10^{-9} to 1.60×10^{-9} N. We calculated the electrical current yielded by the external force using the following equation:

$$\vec{j}^{\alpha} = \sum_i e z_i \vec{v}_i^{\alpha}, \quad (\alpha = +, -), \tag{3}$$

where e is the elementary charge, z_i is the charge of ion i and $\vec{v}_i$ is the velocity of the centre of mass of ion i. The electrical conductivity of the cations and anions, which was referred to as the partial electrical conductivity, was estimated as

$$\sigma^{\alpha} = \frac{\vec{j}^{\alpha}}{V\vec{E}}, \tag{4}$$

where $\vec{E}$ is the electric field and V is the volume of the simulation cell. Figures 7 and 8 show the results of the electric current and the partial electrical conductivity, respectively. We should note that the electric current was not directly proportional to the magnitude of the external field. In simple Coulomb liquids such as molten salts, the electric current and the magnitude of the external field are in direct proportion [17,18]. This nonlinear effect of the electric current is one of the most interesting properties of ionic liquids. The nonlinear effect is caused by the large occupied volume and the flexibility of the cation. The total electrical conductivity is the sum of each of the partial conductivities ($\sigma = \sigma^+ + \sigma^-$). Tables 2 and 3 list the total and the partial electrical conductivities. The electrical conductivity of [bmim]NO_3 are larger than that of [bmim]PF_6. This tendency is the same as the results of the diffusion constants and the reason for this is also not clarified from the structural results. A possibility is the shape effect of NO_3. The configuration of atoms is planar in NO_3 and their effective volume must be smaller than that of [bmim]PF_6. Then, the dynamics of [bmim]NO_3 might be more active than that of [bmim]PF_6. The frequency dependence of the AC electrical conductivity of

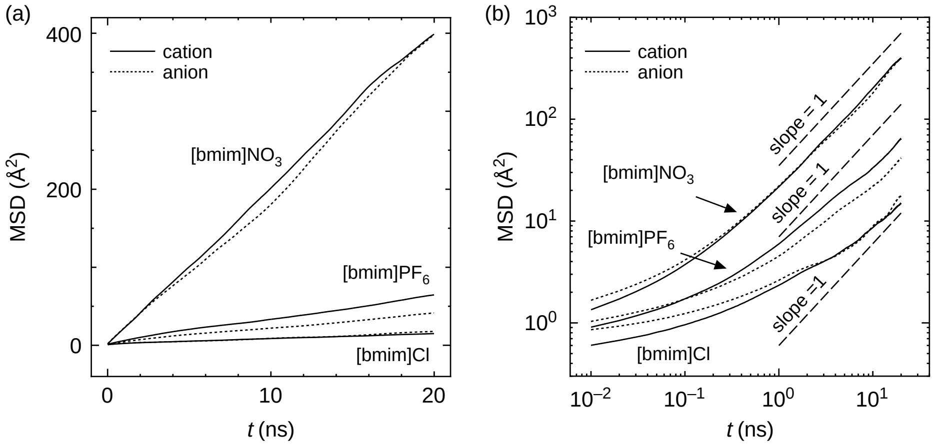

Figure 6. (a) MSDs of [bmim]PF$_6$, [bmim]NO$_3$ and [bmim]Cl and (b) their log–log plot with the lines of slope 1.

Table 1. Diffusion constants of [bmim]PF$_6$, [bmim]NO$_3$ and [bmim]Cl.

	D (10^{-12} m^2/s)	
	Cation	Anion
[bmim]PF$_6$	4.82	3.01
[bmim]NO$_3$	34.1	34.1
[bmim]Cl	1.15	1.91

[bmim]PF$_6$ was derived from experimental data [19]. In their results, the frequency dependence of the electrical conductivity was very large. Their results were consistent with our results.

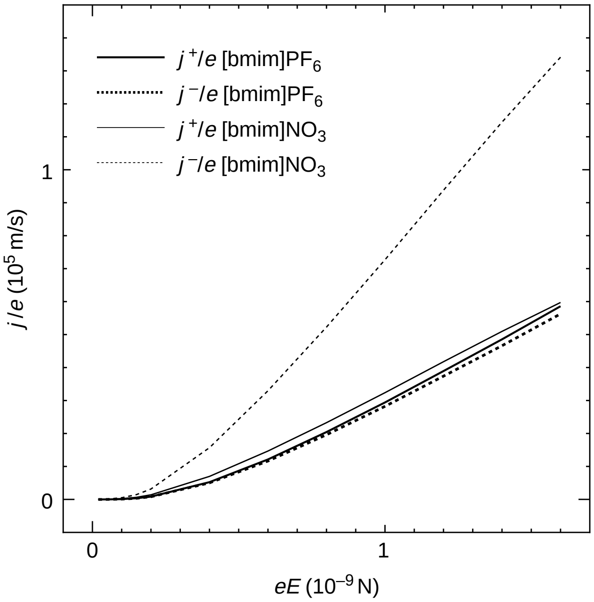

Figure 7. Electric currents of [bmim]PF$_6$ and [bmim]NO$_3$.

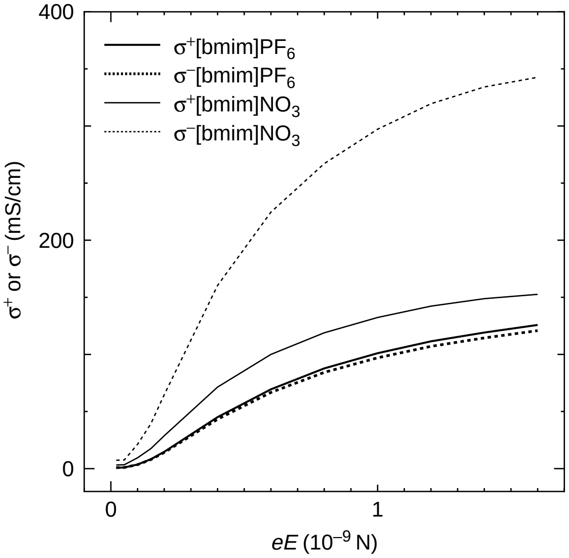

Figure 8. Partial conductivities of [bmim]PF$_6$ and [bmim]NO$_3$.

Table 2. Magnitude of external field dependences of total and partial electrical conductivity of [bmim]PF$_6$.

eE	σ^+ (mS/cm)	σ^- (mS/cm)	σ (mS/cm)
0.02	0.85	0.90	1.75
0.20	14.7	14.2	28.9
1.00	101.1	97.1	198.1
1.60	125.8	120.9	246.7

4. Summary

The structures of [bmim]PF$_6$ at 216 and 4096 ion pairs were almost the same. The size effect of the structure was not large. It was difficult to obtain an accurate diffusion constant in the small system because the fluctuation of the MSD is very large. A larger and longer simulation is required to estimate the diffusion constant in the slower

Table 3. Magnitude of external field dependences of total and partial electrical conductivity of [bmim]NO_3.

eE	σ^+ (mS/cm)	σ^- (mS/cm)	σ (mS/cm)
0.02	3.23	7.36	10.6
0.20	28.8	64.7	93.5
1.00	132.4	297.2	429.6
1.60	152.6	342.7	495.3

dynamics system. The relationship between the ionic current and the external field strength is nonlinear. Then, the DC electrical conductivity depends on the external field strength. In general, the DC electrical conductivity is constant with the external field strength in typical molten salts [17,18]. This nonlinear effect is one of the most peculiar properties of ionic liquids.

Acknowledgements

This work was supported by Grant-in-Aid (KAKENHI) for Young Scientists (B).

References

[1] J.N. Canongia Lopes, J. Deschamps, and A.A.H. Padua, *Modeling ionic liquids using a systematic all-atom force field*, J. Phys. Chem. B 108 (2004), pp. 2038–2047.

[2] Y. Shim, M.Y. Cho, and H.J. Kim, *A molecular dynamics computer simulation study of room-temperature ionic liquids. I. Equilibrium solvation structure and free energetics*, J. Chem. Phys. 122 (2005), pp. 044510 1–12.

[3] S. Alavi and D.L. Thompson, *Molecular dynamics studies of melting and some liquid-state properties of 1-ethyl-3-methylimidazolium hexafluorophosphate [emim]*PF_6, J. Chem. Phys. 122 (2005), pp. 154704 1–12.

[4] X. Wu, Z. Liu, S. Huang, and W. Wang, *Molecular dynamics simulation of room-temperature ionic liquid mixture of [bmim]*[BF_4] *and acetonitrile by a refined force field*, Phys. Chem. Chem. Phys. 7 (2005), pp. 2771–2779.

[5] T.I. Morrow and E.J. Maginn, *Molecular dynamics study of the ionic liquid 1-n-butyl-3-methylimidazolium hexafluorophosphate*, J. Phys. Chem. B 106 (2002), pp. 12807–12813.

[6] T. Yan, C.J. Burnham, M.G.D. Popolo, and G.A. Voth, *Molecular dynamics simulation of ionic liquids: The effect of electronic polarizability*, J. Phys. Chem. B 106 (2004), pp. 11877–11881.

[7] J. Picalek and J. Kolafa, *Molecular dynamics study of conductivity of ionic liquids: The Kohlrausch law*, J. Mol. Liq. 134 (2007), pp. 29–33.

[8] M.G. Del Pópolo and G.A. Voth, *On the structure and dynamics of ionic liquids*, J. Phys. Chem. B 108 (2003), pp. 1744–1752.

[9] S. Tsuzuki, W. Shinoda, H. Saito, M. Mikami, H. Tokuda, and M. Watanabe, *Molecular dynamics simulations of ionic liquids: Cation and anion dependence of self-diffusion coefficients of ions*, J. Phys. Chem. B 113 (2009), pp. 10641–10649.

[10] M.H. Kowsari, S. Alavi, M. Ashrafizaadeh, and B. Najafi, *Molecular dynamics simulation of imidazolium-based ionic liquids. I. Dynamics and diffusion coefficient*, J. Chem. Phys. 129 (2008), pp. 224508 1–13.

[11] M.H. Kowsari, S. Alavi, M. Ashrafizaadeh, and B. Najafi, *Molecular dynamics simulation of imidazolium-based ionic liquids. II. Transport coefficients*, J. Chem. Phys. 130 (2009), pp. 014703 1–10.

[12] M. Taiji, T. Narumi, Y. Ohno, N. Futatsugi, A. Suenaga, N. Takada, and A. Konagaya, *Protein explorer: A petaflops special-purpose computer system for molecular dynamics simulations*, Proceedings of the SC2003 (High Performance Networking and Computing), CDROM, Phoenix, AZ, 2003.

[13] M. Taiji, *MDGRAPE-3 chip: A 165-Gflops application-specific LSI for molecular dynamics simulations*, HOT CHIPS 16, Stanford, CA, USA, August 2004.

[14] T. Narumi, Y. Ohno, N. Okimoto, T. Koishi, A. Suenaga, N. Futatsugi, R. Yanai, R. Himeno, S. Fujikawa, M. Ikei, and M. Taiji, *A 55 TFLOPS simulation of amyloid-forming peptides from yeast prion Sup35 with the special-purpose computer system MDGRAPE-3*, Proceedings of the SC06 (High Performance Computing, Networking, Storage and Analysis), CDROM, Tampa, FL, 2006.

[15] M.E. Tuckerman, B.J. Berne, and G.J. Martyna, *Reversible multiple time scale molecular dynamics*, J. Chem. Phys. 97 (1992), pp. 1990–2001.

[16] N. Matsubayashi and M. Nakahara, *Reversible molecular dynamics for rigid bodies and hybrid Monte Carlo*, J. Chem. Phys. 110 (1999), pp. 3291–3301.

[17] T. Koishi, Y. Arai, Y. Shirakawa, and S. Tamaki, *Transport coefficients in molten NaCl by computer simulation*, J. Phys. Soc. Jpn. 66 (1997), pp. 3188–3193.

[18] T. Koishi and S. Tamaki, *Partial conductivities of a molten salt based on Langevin equation*, J. Phys. Soc. Jpn. 68 (1999), pp. 964–971.

[19] A. Rivera, A. Brodin, A. Pugachev, and E.A. Rössler, *Orientational and translational dynamics in room temperature ionic liquids*, J. Chem. Phys. 126 (2007), pp. 114503 1–7.